Discover Oncology

Research

Anticancer potential of eugenol in hepatocellular carcinoma through modulation of oxidative stress, inflammation, apoptosis, and proliferation mechanisms

Mohamed Y. Zaky[1] · Hadeer M. Morsy[1] · Adel Abdel-Moneim[1] · Khairy M. A. Zoheir[2] · Anthony Bragoli[3] · Mostafa A. Abdel-Maksoud[4] · Abdulaziz Alamri[4] · Osama M. Ahmed[1]

Received: 18 December 2024 / Accepted: 26 March 2025
Published online: 12 June 2025

Abstract
This investigation explored the chemopreventive effects of eugenol on diethylnitrosamine (DENA) and acetylaminofluorene (AAF)-induced hepatocellular carcinoma (HCC) in Wistar rats. To induce HCC, DENA was administered intraperitoneally once per week for two weeks at a concentration of 150 mg/kg body weight (b.w.), followed by oral AAF administration for 3 weeks, four times a week, at a dosage of 20 mg/kg b.w. After these three weeks, the rats were treated with eugenol every other day for 17 weeks at a dosage of 20 mg/kg b.w. In vitro, eugenol reduced cell viability (IC50 of 189.29 µg/mL) and inhibited cell migration in the HCC cell line HepG2. Moreover, eugenol treatment in DENA/AAF-induced rats significantly improved cancerous histopathological changes and reduced inflammatory cell infiltration in the liver. Eugenol treatment significantly reduced the activity levels of alanine aminotransferase (ALT), aspartate aminotransferase (AST), and alkaline phosphatase (ALP), along with the levels of total bilirubin (TBIL), alpha-fetoprotein (AFP), carcinoembryonic antigen (CEA), carbohydrate antigen 19–9 (CA 19–9), lipid peroxides (LPO), tumor necrosis factor-α (TNF-α), and interleukin-1β (IL-1β). Additionally, the expressions of nuclear factor kappa-light-chain-enhancer of activated B cells (NF-κB), interleukin-8, C-X-C Motif Chemokine Receptor 3 (CXCR3), B-cell lymphoma 2 (Bcl-2), IQ Motif Containing GTPase Activating Protein 1 (IQGAP1), IQ Motif Containing GTPase Activating Protein 3 (IQGAP3), Harvey rat sarcoma viral oncogene homolog (HRAS), Kirsten rat sarcoma viral oncogene homolog (KRAS), and Ki-67 were downregulated following eugenol administration in DENA/AAF-induced HCC. Conversely, eugenol supplementation significantly enhanced glutathione (GSH) content, as well as the activities of glutathione peroxidase (GPx) and superoxide dismutase (SOD), and the levels of nuclear factor erythroid 2-related factor 2 (Nrf2). Furthermore, the expressions of tumor suppressor gene p53, Bcl-2-associated X protein (BAX), death receptor 4 (DR4), death receptor 5 (DR5), decoy receptor 1 (DcR1), programmed cell death 5 (PDCD5), and IQ Motif Containing GTPase Activating Protein 2 (IQGAP2) were markedly upregulated compared to the DENA/AAF-administered group. These findings indicate that the potent anticancer effects of eugenol are primarily driven by its ability to reduce oxidative stress, suppress inflammation, and inhibit cell proliferation while promoting apoptosis. This study underscores the potential of eugenol as a promising therapeutic agent for the prevention and management of HCC, offering a novel approach to HCC treatment.

✉ Mohamed Y. Zaky, mohamedzaki448@science.bsu.edu.eg; ✉ Osama M. Ahmed, osamamoha@yahoo.com; Hadeer M. Morsy, hadeermuhammed1234@gmail.com; Adel Abdel-Moneim, adel.hassan@science.bsu.edu.eg; Khairy M. A. Zoheir, khma25@gmail.com; Anthony Bragoli, ANB562@pitt.edu; Mostafa A. Abdel-Maksoud, mabdmaksoud@ksu.edu.sa; Abdulaziz Alamri, abalamri@ksu.edu.sa | [1]Molecular Physiology Division, Zoology Department, Faculty of Science, Beni-Suef University, P.O.Box 62521, Beni-Suef, Egypt. [2]Cell Biology Department, Biotechnology Research Institute, National Research Centre, Cairo 12622, Egypt. [3]Department of Immunology, University of Pittsburgh School of Medicine, Pittsburgh, PA, USA. [4]Biochemistry Department, College of Science, King Saud University, P.O. Box 10219, 11433 Riyad, Saudi Arabia.

Keywords Hepatocellular carcinoma · Diethylnitrosamine · Acetylaminofluorene · Eugenol · Oxidative stress

Abbreviations

AAF	Acetylaminofluorene
Ab	Apoptotic blebs
AC	Apoptotic cells
AFP	Alpha fetoprotein
ALP	Alkaline phosphatase
ALT	Alanine transaminase
AST	Aspartate transaminase
b.w.	Body weight
Bax	BCL2 Associated X
Bcl-2	B cell lymphoma/ leukemia 2
BC	Binucleated cells
BD	Bile duct
BV	Congested blood vessels
C	Tumor cells in the form of cords
CA19.9	Cancer antigen 19.9 or carbohydrate antigen 19.9
cDNA	Complementary DNA
CEA	Carcinoembryonic antigen
CXCR3	CXC chemokine receptor family
DcR1	Decoy receptor 1
DENA	Diethylnitrosamine
DMSO	Dimethyl sulfoxide
DR4	Death receptor 4
DR5	Death receptor 5
GPx	Glutathione peroxidase
GSH	Reduced glutathione
HCC	Hepatocellular carcinoma
HepG2	Human liver cancer cell line
HRAS	Harvey rat sarcoma viral oncogene homolog
IC50	Inhibitory concentration
IF	Inflammatory cell infiltrations
IL-1β	Interleukin 1 beta
IL-8	Interleukin 8
IQGAP1	IQ-domain GTPase-activated protein 1
IQGAP2	IQ-domain GTPase-activated protein 2
IQGAP3	IQ-domain GTPase-activated protein 3
Ki-67	Antigen ki-67
KRAS	Kirsten ras oncogene homolog
LPO	Lipid perioxidation
MC	Multinucleated cells
MTT	3-(4,5-Dimethylthiazol-2-yl)-2,5-diphenyl tetrazolium bromide
N	Tumor nests
Nc	Necrosis
NF-κB	Nuclear factor kappa-light-chain enhancer of activated B cells
Nrf2	Nuclear factor erythroid 2-related factor 2
P	Pyknotic nucleoli
p53	Tumor suppressor gene 53
PDCD5	Programmed cell death protein 5
PV	Portal vein

ROS	Reactive oxygen species
S	Sinusoids
SE	Standard error
Se	Growing septa
SOD	Superoxide dismutase
SR	Hepatocytes forming signet ring
SPSS	Statistical product and service solutions
T	Tumor cells arranged in trabeculae
TBST	Tris-buffered saline containing Tween20
TNF-α	α-Tumor necrosis factor-α
T.bilirubin	Total bilirubin

1 Introduction

Hepatocellular carcinoma (HCC) is one of the most prevalent causes of cancer death globally [1]. In Egypt, HCC is the fourth most common cancer and has the second highest fatality rate among cancers [2]. It typically occurs when the liver is chronically damaged, often due to liver fibrosis [3]. The most prevalent triggers of HCC include hepatitis C and hepatitis B virus, chemical carcinogens, air pollutants, and dietary additives [4]. Novel therapies are constantly being developed to fight against this fatal disease [5].

Diethylnitrosamine (DENA) is a carcinogenic compound that provokes cancers in numerous organs, including the lungs and the liver [6, 7], and has been used extensively for this purpose in experimental animals [8]. It can also be coupled with other carcinogens like acetylaminofluorene (AAF), which functions like a promoter for several oncogenes 5. It is a part of many different foods, including soybeans, cheese, salted, smoked, and dried fish, alcoholic beverages, and cured meat [9].

Both oxidative stress and inflammation play key roles in the progression of HCC [10]. High concentrations of reactive oxygen species (ROS) are associated with DNA damage, leading to genetic instability, enhanced cell survival, migration, and pro-tumorigenic signaling in HCC cells [11, 12]. Furthermore, oxidative stress induces a chronic inflammatory response, which contributes to tissue damage and sustains an inflammatory microenvironment, further promoting HCC progression [13].

The pathophysiology of HCC is primarily driven by two key processes: cell migration and apoptosis, particularly within tumor cells [14]. Cell migration plays a crucial role in the spread and metastasis of HCC, facilitating the invasion of surrounding tissues and the formation of secondary tumors. Apoptosis is essential for controlling HCC growth; triggering apoptosis can eliminate cancer cells, while deficiencies in apoptotic signaling can lead to 'drug-resistant' tumor cells. This dysregulation of apoptosis contributes significantly to the progression of HCC, especially in the context of chronic liver disease, cirrhosis, and the subsequent development of HCC [15].

Consequently, novel therapeutic strategies are needed to restrict the development of advanced HCC [16, 17]. Various medicinal plants have been prescribed to cancer patients as alternative medicines to both inhibit and remedy the disease. Besides their powerful chemoprotective and anticarcinogenic properties, these plants also possess anti-proliferative and anticancer chemicals that are less toxic than those in conventional therapies [18].

One such medicinal plant with anti-cancer properties is cloves. Cloves were conventionally used in medicine because of their numerous health benefits and an abundance of biologically active secondary metabolites [19]. Eugenol, the major phenolic ingredient of clove essential oil, is a remarkable multifunctional phytochemical with various medicinal activities, including being anticarcinogenic, antioxidant, and anti-inflammatory [20, 21]. Its anticancer effect has been demonstrated in liver cancer [22] and breast cancer [23]; however, its effects on the DENA/AAF-induced liver cancer model are poorly understood.

Thus, the goal of this research was to explore the prospective chemopreventive and anticancer effects of eugenol against DENA/AAF-induced HCC. Further, we aimed to elucidate its mechanisms of action and its effects on cell proliferation, oxidative stress, antioxidant defense, inflammation and apoptosis.

2 Material and methods

2.1 Chemicals and reagents

DENA, AAF, and eugenol were purchased from Sigma-Aldrich Chemicals Co. (St. Louis, MO, USA) and were stored at 2–4 °C, excluding eugenol, which was kept at 37 °C. The activities of alanine transaminase (ALT) (0184), aspartate transaminase (AST) (0152), and alkaline phosphatase (ALP) (21,002) were determined using chemical kits from Biosystem S. A. (Spain). Total bilirubin (202,159) was detected colorimetrically using Diamond Diagnostic Kits (Badr City, Cairo, Egypt). Albumin (21,008) was determined by reagent kits purchased from HUMAN Gesellschaft für Biochemica and Diagnostica mbH, (Wiesbaden, Germany). ELISA kits provided by R&D Systems (USA) were utilized to assess levels of serum alpha-fetoprotein (AFP) (MBS267612), carcinoembryonic antigen (CEA) (MBS720630), and carbohydrate antigen 19.9 (CA19.9) (MBS2515823). The additional reagents utilized in the experiments and examinations were of quality for analysis.

2.2 Cell lines and cell culture

HepG2 was purchased from ATCC (American Type Culture Collection). It was previously used to determine the viability of cells, as described in Yassin et al. [24], using the 3-(4,5-dimethylthiazol-2-yl)-2,5-diphenyl tetrazolium bromide-based assay (MTT, Serva Electrophoresis, Germany). The reagent is broken down by viable cells to give a purple-colored product. The cytotoxic effect was studied using the MTT assay by exposing cells to varied doses of eugenol (0, 78.125, 156.25, 312.5, 625, 1250, 2500, and 5000 µg/mL) in 0.1% (v/v) dimethyl sulfoxide (DMSO, SDFCL, Mumbai-30) for 24 h. Controls that are not positive were exposed alone to 0.1% (v/v) DMSO. Incubation of dead cells for 4 h at 37 °C in a 5% CO_2 incubator after rinsing off with sterile phosphate-buffered saline. The intra-cytoplasmic MTT formazan crystals were dissolved in 100 µL DMSO. At 590 nm, the optical density was observed on a microplate reader (SunRise, TECAN, Inc, USA) to estimate the number of cells that survive, and the viability percentage was determined as $[(ODt/ODc)] \times 100\%$, where ODt is the mean optical density of treated cells, and the mean optical density of untreated cells is denoted by ODc. The 50% inhibitory concentration (IC50), which is the concentration needed to cause negative consequences in 50% of undamaged cells [25].

2.3 Wound healing assay

The Wound healing assay of HepG2 cell culture was determined according to the method described in Martinotti and Ranzato [26]. Briefly, cells were seeded in 6-well plates and cultured to confluence. A sterile 200 µL pipette tip was used to create a linear scratch wound across the cell monolayer. After wounding, the cells were washed with PBS to remove debris, and fresh medium was added. Images of the wound area were captured 72 h post-scratch using a phase contrast microscope. For quantification of the distance cells migrated into the wound, three random sites across the scratch per well were measured from the captured images.

2.4 Animals and experimental design

Mature adults male Wistar rats 8–9 weeks' old about 100–120 g weight was utilized in our investigation. The rats were transported at Helwan Station in Cairo, Egypt, by the Egyptian Biological Products and Vaccines Organization (VACSERA). Maintaining of in cages for 14 days before the experiment to ensure no concurrent infections. Keeping the rats in well-aerated polypropylene crates and housed in the Zoology Department, Faculty of Science, Beni-Suef University, Egypt. They were maintained on an orderly diurnal illumination cycle (10–12 h/day) at room temperature (20–25 °C) with regular food and water supply. The Animal Rescue and Use Committee of the Faculty of Science, Beni-Suef University, Egypt, approved all experimental techniques and the research strategy (Approval Number: BSU/FS/2019/3). All safety protocols were implemented, and every effort was made to minimize the number of animals used, as well as their suffering, discomfort, and distress. All methods were performed in accordance with the relevant ethical guidelines and regulations for animal research. The Animal Rescue and Use Committee of the Faculty of Science, Beni-Suef University, Egypt, permits a maximal tumor size of 2 cm in diameter for animal studies. During this study, the tumor size was strictly monitored and did not exceed this limit, ensuring compliance with ethical guidelines.

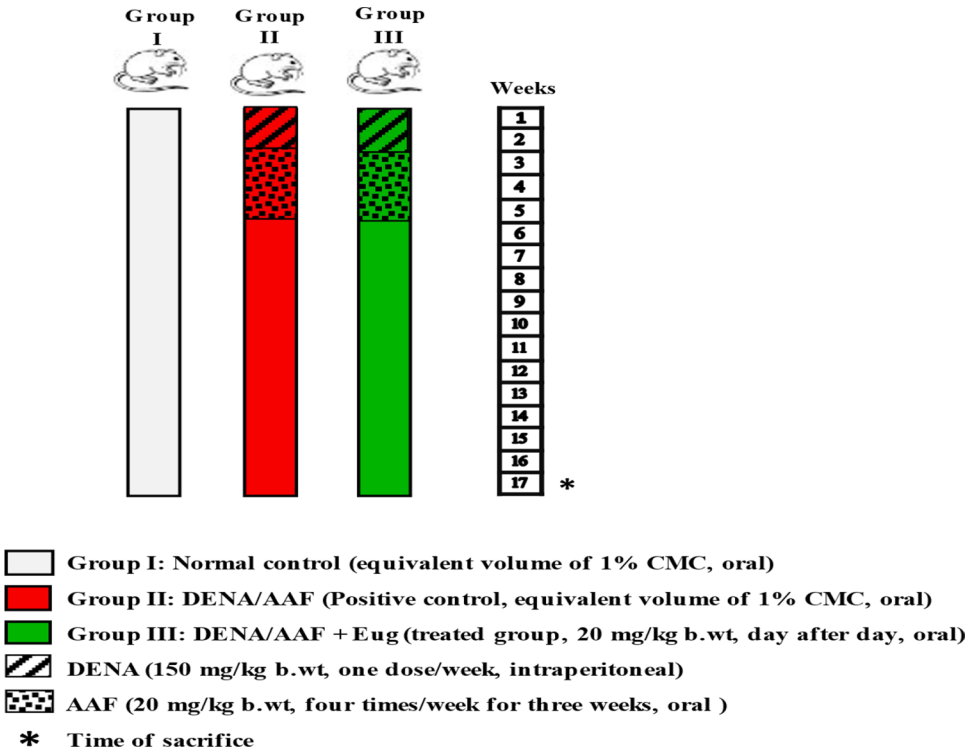

Fig. 1 DENA, AAF, and eugenol administration experimental design

Thirty mature male Wistar rats were separated into 3 groups of 10 rats (Fig. 1) each. Group I served as the negative control (normal control group). The other 2 groups were given DENA at 150 mg/kg body weight (b.w.) intraperitoneally once per week for 2 weeks, followed by an oral AAF dosage at 20 mg/kg b.w. four different times per week for 3 weeks [27]. Group II was presented only DENA/AAF and served as the positive control, while group III was administered eugenol (dissolved in 1% carboxymethyl cellulose) orally at 20 mg/kg b.w. every alternate day for 17 weeks [28] on top of the DENA/AAF regimen.

2.5 Sample collections

The rats were sacrificed after 17 weeks using inhalation anesthesia. Specifically, the animals were placed in a chamber with an appropriate anesthetic gas (e.g., isoflurane), and once fully anesthetized, they were humanely euthanized following standard protocols. After dissection and subsequent decapitation, samples of blood were gained from the jugular vein and liver tissue samples were enucleated for biochemical, molecular, and histological analyses. After permitting the blood samples for making coagulation at 37 °C, they were centrifuged for 15 min at 3000 rpm. The supernatant sera were separated with a Pasteur pipette and stored at − 20 °C in sterile tubes. Glaciated liver tissue (1 g) was melted, lysed in ice-cold water, and homogenized in 10 mL of 0.9% NaCl to yield a homogenate (w/v) of 1% homogenate (w/v). The liver homogenates were centrifuged at 3000 rpm for 15 min. Liver slices (3 mm^3) were preserved at − 70 °C in sterile Eppendorf tubes until they were utilized for RNA isolation and real-time PCR analysis.

2.6 Serum biochemical assessment

The sera levels of ALT [29], AST [29], ALP [30], total bilirubin [31], Albumin [32] were estimated. The levels of AFP, CEA and CA19.9 were assessed as per the instructions from the manufacturer utilizing ELISA kits provided by R&D Systems (USA).

2.7 Hepatic oxidative/antioxidant assessment

Hepatic lipid peroxides (LPO) (MD 25 28), reduced glutathione (GSH) (GR 25 10), and the activities of antioxidant enzymes like GSH peroxidase (GPx) (GP 2524) and superoxide dismutase (SOD) (SD 25 20) were colorimetrically quantified using

Bio-Diagnostic Kits (Dokki, Giza, Egypt), as per the Ohkawa et al. [33], Beutler et al. [34], Paglia and Valentine [35], and Nishikimi et al. [36], respectively.

Liver tumor necrosis factor-α (TNF-α) (CSB-E11987r) was tested by the quantitative sandwich enzyme immunoassay technique using kits from R&D Systems (USA). Interleukin-1β (IL-1β) (# MBS825017) was determined using the Ray Biotech ELISA Kit (USA), and the transcriptional activity of nuclear factor erythroid 2-related factor 2 (Nrf2) (MBS752046) was calculated by ELISA using the Nrf2 Transcription Factor Examination Kit (Abcam, Cambridge, UK). All reagents were used as per the instructions from the manufacturer.

2.8 Western blotting for Ki-67

As previously described, western blotting was performed to assess the expression of Ki-67 in the liver [37]. For total protein extraction from liver tissue samples, a ReadyPrep™ protein extraction kit (cat #163–2086, Bio-Rad Inc.) was utilized accordance to the company's recommendations. Protein was quantified using a Bradford assay kit (SK3041; Bio Basic Inc., Markham, Ontario L3R 8T4 Canada), separated by 10% SDS-PAGE (Bio-Rad Laboratories, Inc. cat #161-0181), and transferred to PDVF membranes. Membranes were then blocked with 5% skim milk dissolved in Tris-buffered saline containing Tween20 (TBST). The membranes were then treated with the appropriate primary antibodies against Ki-67 and β-actin overnight at 4 C. The membranes were probed with HRP-conjugated secondary antibodies (Goat anti-rabbit IgG- HRP-1 mg Goat mab, Novus Biologicals) and generated utilizing a chemiluminescent substrate (Clarity™ Western ECL substrate, Bio-Rad cat#170-5060). Image analysis software was utilized on the ChemiDoc MP imager Using protein normalization, measure the band intensity of targeted proteins against the control sample beta-actin (housekeeping protein).

2.9 RT-qPCR

Total RNA has been obtained from liver tissues as directed by the manufacturer using the TRIzol reagent (Invitrogen). By calculating the absorbance at 260 nm and calculating the 260/280 ratio, the concentration and purity of the isolated RNA were calculated. Complementary DNA (cDNA) synthesis was performed out according to the manufacturer's instructions using a High-Capacity cDNA Reverse Transcription Kit (A32702, Applied Biosystems). As an internal control, GAPDH was used. The following quantitative studies of target gene mRNA expression were performed on the ABI Prism 7500 System (Applied Biosystems): A cDNA synthesis kit was used to convert 1 g RNA into cDNA (Thermo Scientific). Table 1 showed the genes primer sequences tested. The QuantStudio™ 7 Flex Real-Time PCR System (Thermo Scientific) was used to run real-time PCR with PowerUp™ SYBR® Green Master Mix (Thermo Scientific). The relative expression of distinct genes was calculated using the $2^{-\Delta\Delta CT}$ method. The data are reported as the gene expression fold change relative to a calibrator and normalized to the internal control.

2.10 Histopathology study

Post 17 weeks, every rat's liver was dissected out. Minor liver sections from each rat were settled in 10% neutral-buffered formalin for 24 h. The sections were clarified, encased in paraffin in a hot air stove at 56 °C for 24 h, and passed on 70% alcohol for histopathological analysis. The paraffin wax tissue blocks were cut at a thickness of 5 µm. The tissue samples have been stained with hematoxylin and eosin [38] and for examination, a light microscope with a camera was used. Additionally, the histopathological scores of liver lesions in the normal control group, DENA/AAF-administered group, and DENA/AAF-administered, eugenol-treated group were determined using a scoring system based on lesion grades as follows: 0 refers to no lesion, I refers to mild, II refers to moderate, and III refers to severe.

2.11 Statistical analysis

The results were measured using SPSS version 20 (SPSS 2011). The data are provided in the form of mean ± standard error (SE). Duncan's technique for post-hoc analysis was utilized for comparing statistics. $p < 0.05$ was thought to be statistically significant.

Table 1 The primer sequences used in this study

mRNA species	GenBank accession number	Primer sequence 5′–3′
NF-κB	NM_001276711.1	F: 5′TTCAACATGGCAGACGACGA3′ R: 5′TGCTCTAGTATTTGAAGGTATGGG3′
IL-8	X77797.1	F: 5′CAGAGACTTGGGAGCCACTC3′ R: 5′CAGAGTAAAGGGCGGGTCAG3′
CXCR3	NM_053415.1	F: 5′GCTCTTTGCCCTCCCAGATT3′ R: 5′TCCACATGGCTTTCTCGACC3′
Bcl-2	NM_016993.2	F: 5′GGGGCTACGAGTGGGATACT3′ R: 5′GACGGTAGCGACGAGAGAAG3′
Bax	NM_017059.2	F: 5′AGACACCTGAGCTGACCTTG3′ R: 5′GTTGTTGTCCAGTTCATCGCC3′
p53	AH010014.2	F: 5′GTTTTTGTTCCTGAGCCCCG3′ R: 5′GAGCAAGGGGTGACTTTGGG3′
DR4	NM_003844.3	F: 5′ATGAACTCACTGGTTTCTTGGC3′ R: 5′TTCGCGTCCGGCTTCCTCAAG3′
DR5	NM_001395720.1	F: 5′GGCCTCGGTCATATCAGTGG3′ R: 5′GCACCTAGCAGGTGGTTGAT3′
DCR1	NC_003281.10	F: 5′GCTGAAGAGACAATGAAC3′ R: 5′ACGATCACAAGGAGGAAG3′
PDCD5	NM_001106247.1	F: 5′TGAAGCGATTCCAACCGAGT3′ R: 5′GCTCCGTGGGTCTGTCTAAG3′
IQGAP1	NM_001108489.1	F: 5′GCGGCTTCCAACAAGATGTTT3′ R: 5′CAGCAGTTCATGGATGGGGT3′
IQGAP2	XM_039103456.1	F: 5′CACAGTACTGGGTGTGTCCC3′ R: 5′GGAATCTACGGACGCTGGAG3′
IQGAP3	NM_001191709.1	F: 5′AGCCTATGATCGTCTCACAGC3′ R: 5′CACAGGTACTGGTAGGCGAC3′
HRAS	NM_001130441.1	F: 5′TGGCTGGAAGTAGGAGGTGT3′ R: 5′CAGAAGAGAAGGGCTGCACA3′
KRAS	NM_031515.3	F: 5′GACAGGGTGTTGACGATGCC3′ R:5′TGTGCCTTAAGAAAGAGTACAAACT3′
GAPDH	NM_017008.4	F: 5′GCGAGATCCCGCTAACATCA3′ R: 5′ATTCGAGAGAAGGGAGGGCT3′

3 Results

3.1 Cytotoxic effect of eugenol on HepG2

The influence of different eugenol concentrations on percentages of viability of HepG2 cells is depicted in (Fig. 2). The viability progressively decreased as the eugenol concentration elevated (78.125–5000 µg/mL), indicating that the cytotoxic effect was dose-dependent. The IC50 was calculated to be 189.29 ± 1.18 µg/mL.

3.2 Wound healing assay

The data shows that eugenol treatment has an inhibitory effect on wound healing (Fig. 3). The wound healing assay demonstrated that eugenol contributed to reduced cell migration in HepG2 cell culture, as shown 72 h after performing the scratch and incubation. Quantification of wound closure revealed that eugenol significantly ($p < 0.05$) reduced the migration of HepG2 cells compared to the control group. These results suggest that eugenol inhibits cell migration in HepG2 cells.

3.3 Histological changes of liver induced by DENA/AAF

Histological examination of liver tissues from the normal control group revealed normal architecture of hepatocytes with portal vein and bile duct surrounding the hepatic sinusoids and associated with a highly eosinophilic cytoplasm

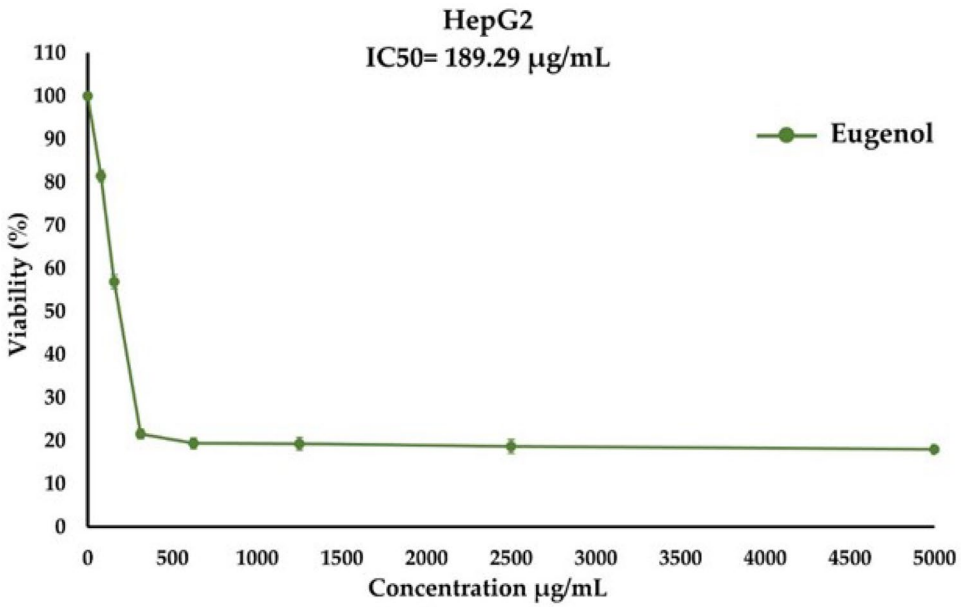

Fig. 2 Effect of different doses of eugenol (0–5000 µg/mL) on the viability of HepG2 cells

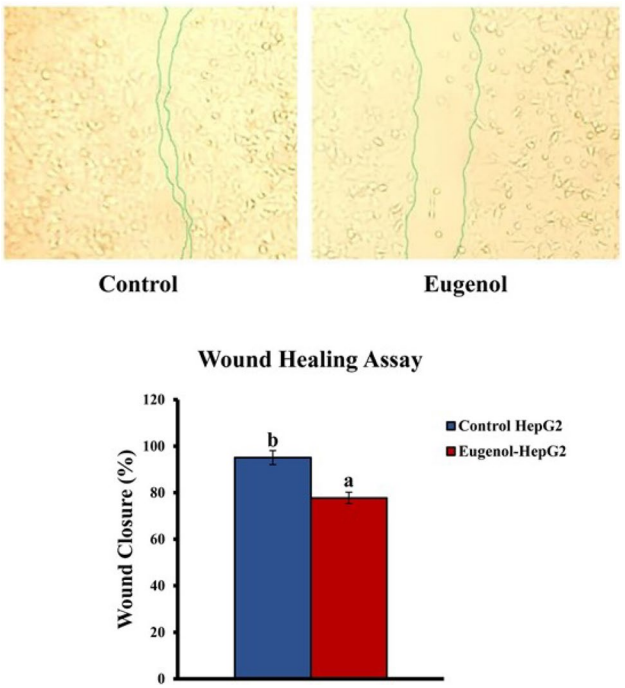

Fig. 3 Effect of eugenol on wound healing assay of HepG2 cell culture after performing the scratch and incubation for 72 h

and distinct nuclei (Fig. 4A). The liver of DENA/AAF-administered rats showed remarkable changes including tumor nests surrounded by fibrous tissue, congested blood vessels, and inflammatory cell infiltration (Fig. 4B). The portal tract was congested and was associated with inflammatory infiltration and necrosis surrounding hepatocytes. Some tumor cells form nests and cords, while others contain bile pigment in their cytoplasm (Fig. 4C). The tumor cells that formed nests had condensed chromatin within disformed nuclei (Fig. 4D). Figure 4E shows activated Kupffer cells in association with dark shrunken nuclei, binucleated and multi-nucleoli hepatocytes and pykonotic nuclei. Severe inflammatory infiltrations and hepatocytes with a signet ring appearance were observed. Some cells were binucleated and apoptotic cells showed eosinophilic cytoplasm and condensed chromatin in their nuclei (Fig. 4F). These alterations were markedly ameliorated in DENA/AAF-administered rats treated with eugenol. The liver architecture and portal tract structure appeared nearly normal. Also, apoptotic cells with blebbing bodies and apoptotic blebs

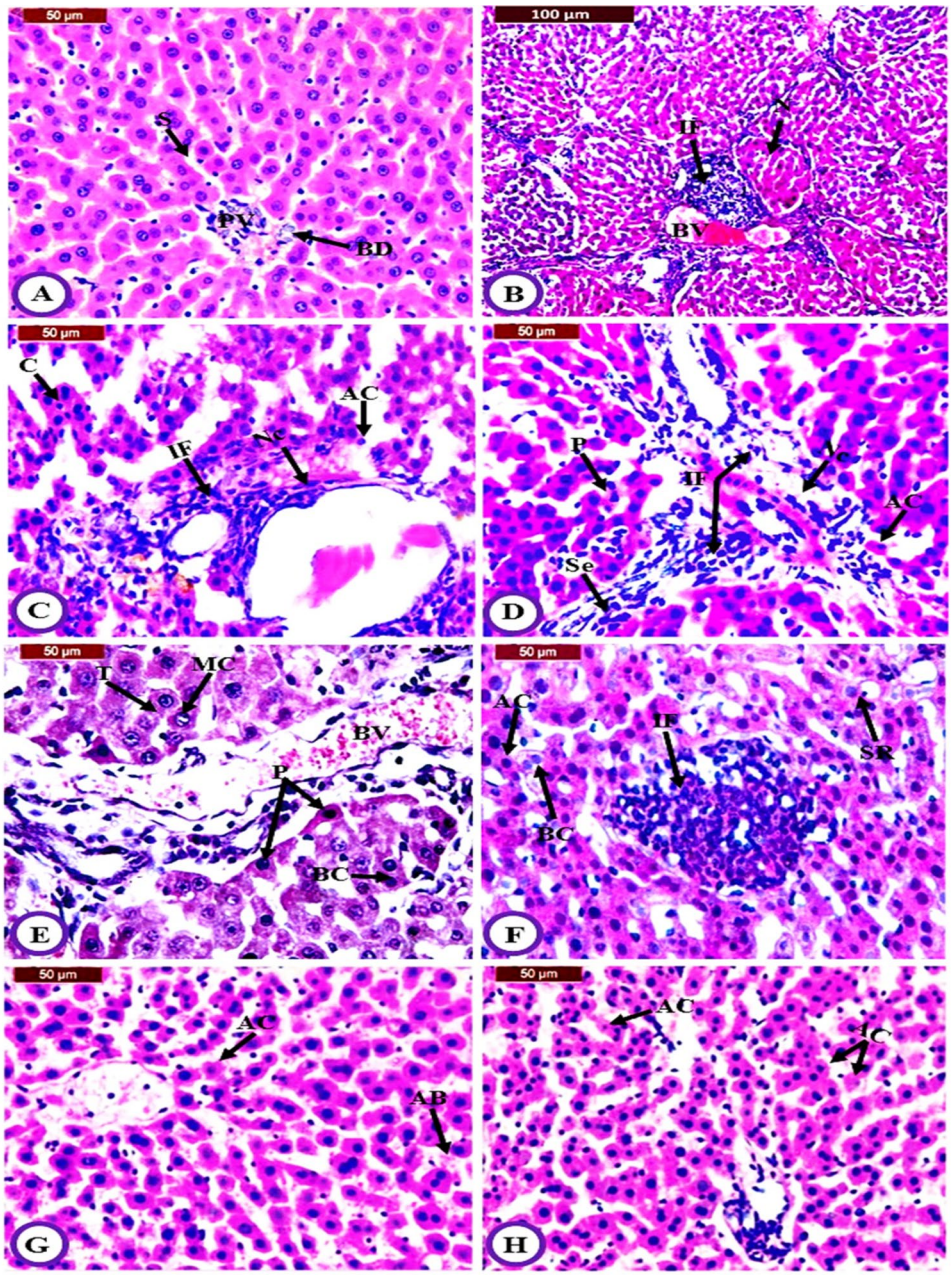

Fig. 4 Photomicrographs from normal liver (**A**, × 400), DENA/AAF-administered rats (**B**, × 100; **C**–**F** × 400) and DENA/AAF-administered rats treated with eugenol (**G** and **H**, × 400). Photomicrograph **A** showing normal liver structure, portal vein (PV), bile duct (BD), and sinusoids (S). Photomicrographs B–F exhibiting several liver cancerous lesions including tumor nests (N), congested blood vessels (BV), inflammatory cell infiltrations (IF), apoptotic cells (AC), necrosis (Nc), growing septa (Se), tumor cells in the form of cords (C), tumor cells arranged in trabeculae (T), binucleated cells (BC), multinucleated cells (MC), hepatocytes forming signet ring (SR), and pyknotic nucleoli (P). Photomicrographs G and H (× 400) demonstrating normal liver architecture and structure and nearly normal portal tract structure. Also, apoptotic cells (AC) and apoptotic blebs (Ab) were observed

were noticed in DENA/AAF-administered rats treated with eugenol (Fig. 4G and H). These histological results from the three groups were assessed by histopathology scores of liver lesions as shown in Table 2.

3.4 Effect on liver function parameters in the serum

Compared with normal control rats, the serum activities of ALT, AST, and ALP, and the total bilirubin level substantially ($p < 0.05$) increased in DENA/AAF-administered rats whereas the albumin level significantly ($p < 0.05$) decreased. Eugenol treatment substantially ($p < 0.05$) lowered the activities of ALT, AST, and ALP, as well as total bilirubin levels. The albumin level increased but the change was non-significant ($p > 0.05$) (Table 3).

Table 2 Histopathological scores of liver lesions in the normal control group, DENA/AAF-administered group, and the DENA/AAF-administered, eugenol-treated group

	Score	Normal control	DENA/AAF	DENA/AAF + Eug
Inflammation	0	6 (100%)	–	3 (50%)
	I	–	1 (16.7%)	2 (33.3%)
	II	–	1 (16.7%)	1 (16.7%)
	III	–	4 (66.6%)	–
Necrosis	0	6 (100%)	1 (16.7%)	6 (100%)
	I	–	2 (33.3%)	–
	II	–	3 (50%)	–
	III	–	–	–
Vascular congestion	0	6 (100%)	–	4 (66.6%)
	I	–	3 (50%)	2 (33.3%)
	II	–	1 (16.7%)	–
	III	–	2 (33.3%)	–
Tumor cells	0	6 (100%)	–	5 (83.3%)
	I	–	3 (50%)	1 (16.7%)
	II	–	3 (50%)	–
	III	–	–	–
Cytoplasmic vacuolization of hepatocytes	0	6 (100%)	–	5 (83.3%)
	I	–	1 (16.7%)	1 (16.7%)
	II	–	3 (50%)	–
	III	–	2 (33.3%)	–
Apoptosis	0	6 (100%)	2 (33.3%)	2 (33.3%)
	I	–	3 (50%)	4 (66.6%)
	II	–	1 (16.7%)	–
	III	–		–

0 refers to no lesion, I refers to mild, II refers to moderate, and III refers to severe. Every group contains 6 rats. The percentage in parentheses represents the rate of animals in each grade

Table 3 Effect of eugenol on serum ALT, AST, and ALP activities, and total bilirubin and albumin levels in DENA/AAF-administered rats

Groups	ALT (U/L)	AST (U/L)	ALP (U/L)	Total bilirubin (mg/dL)	Albumin (g/dL)
Normal control	42.06 ± 3.52^{a}	98.33 ± 1.64^{a}	218.66 ± 1.49^{a}	0.29 ± 0.01^{a}	3.59 ± 0.09^{b}
DENA/AAF	69.20 ± 4.38^{b}	163.16 ± 6.82^{c}	512.00 ± 35.62^{c}	0.97 ± 0.15^{c}	2.98 ± 0.05^{a}
DENA/AAF + Eug	49.96 ± 5.60^{a}	142.16 ± 5.42^{b}	330.00 ± 31.71^{b}	0.62 ± 0.04^{b}	3.15 ± 0.05^{a}

Data are presented as mean (SE). Each group had six samples that were evaluated. Values for parameters that do not possess the same superscript symbol(s) (a, b, and c) were significantly different ($p < 0.05$)

3.5 Effect on serum AFP, CEA, and CA19.9 levels

DENA/AAF injection significantly ($p < 0.05$) increased the serum AFP, CEA, and CA19.9 levels in comparison to normal rats while eugenol treatment substantially ($p < 0.05$) lowered the raised levels of these tumor biomarkers (Table 4).

3.6 Effect on liver oxidative stress and the antioxidant defense system

DENA/AAF-treated rats demonstrated a substantial ($p < 0.05$) raise in the levels of liver LPO as well as a substantial ($p < 0.05$) drop in GSH content as well as GPx and SOD activities, in comparison to normal control rats. The oral dose of eugenol substantially ($p < 0.05$) limited the high level in LPO as well as the drop in GSH content and GPx and SOD activities (Fig. 5).

Table 4 Effect of eugenol on serum AFP, CEA, and CA19.9 levels in DENA/AAF-administered rats

Groups	AFP (ng/mL)	CEA (ng/mL)	CA19.9 (U/L)
Normal control	0.62 ± 0.04^{a}	1.97 ± 0.05^{a}	14.46 ± 0.51^{a}
DENA/AAF	3.93 ± 0.33^{c}	9.16 ± 0.47^{c}	110.73 ± 2.68^{c}
DENA/AAF + Eug	1.74 ± 0.09^{b}	3.93 ± 0.11^{b}	32.63 ± 6.17^{b}

Data are presented as mean (SE). Each group had six samples that were evaluated. Values for parameters that do not possess the same superscript symbol(s) (a, b, and c) were significantly different at $p < 0.05$

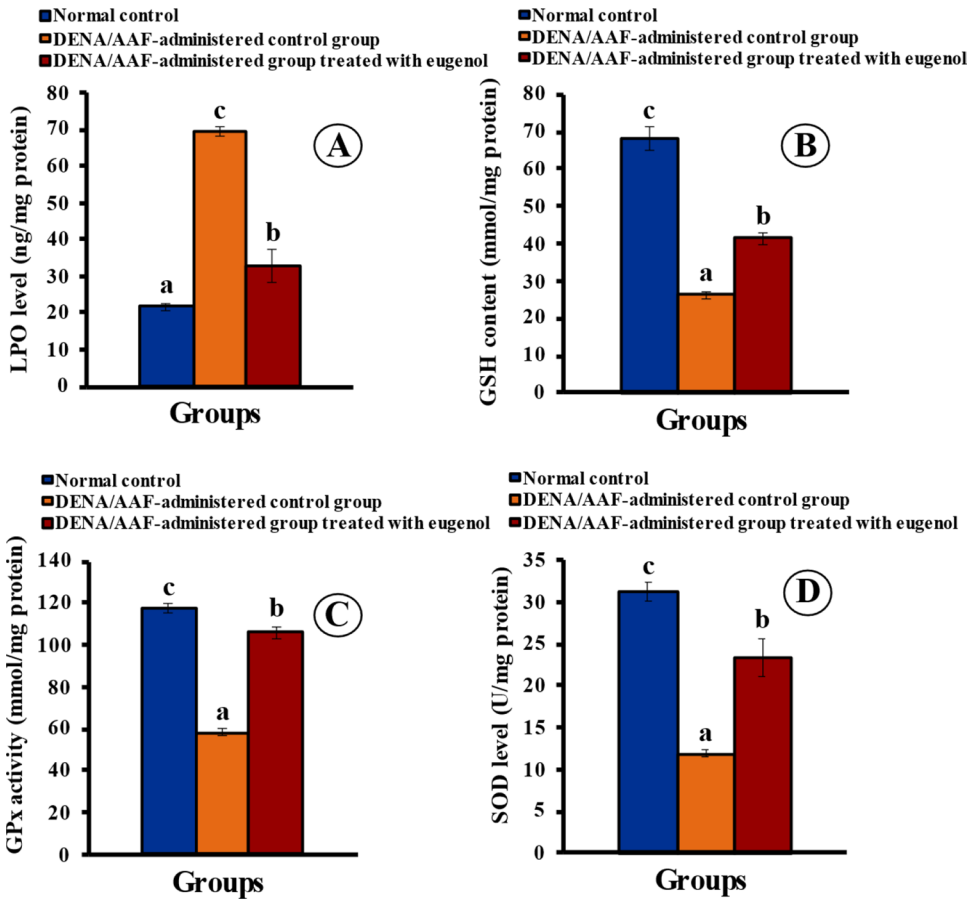

Fig. 5 Effect of eugenol on liver LPO (**A**) level, GSH (**B**) content, and GPx (**C**) and SOD (**D**) activities in DENA/AAF-treated rats. Values and expressed genes that do not have the same symbol(s) (a, b, and c) are significantly different at $p < 0.05$

3.7 Effect on liver inflammation

Administration of DENA/AAF substantially ($p < 0.05$) elevated the levels of liver TNF-α and IL-1β as well as the expression of NF-κB, IL-8, and CXCR3, while substantially reducing Nrf2 levels ($p < 0.05$), in comparison to the normal control rats. Eugenol administration substantially ($p < 0.05$) counteracted these effects (Fig. 6).

3.8 Effect on the expression of apoptosis markers

DENA/AAF-treated rats exhibited substantially ($p < 0.05$) upregulated expression of liver B-cell lymphoma 2 (Bcl-2), and substantially ($p < 0.05$) downregulated expression of tumor suppressor gene 53 (p53), Bcl-2-associated X protein (Bax), death receptor 4 (DR4), death receptor 5 (DR5), decoy receptor 1 (DcR1), and programmed cell death protein 5 (PDCD5). Eugenol treatment significantly ($p < 0.05$) reversed these effects (Fig. 7).

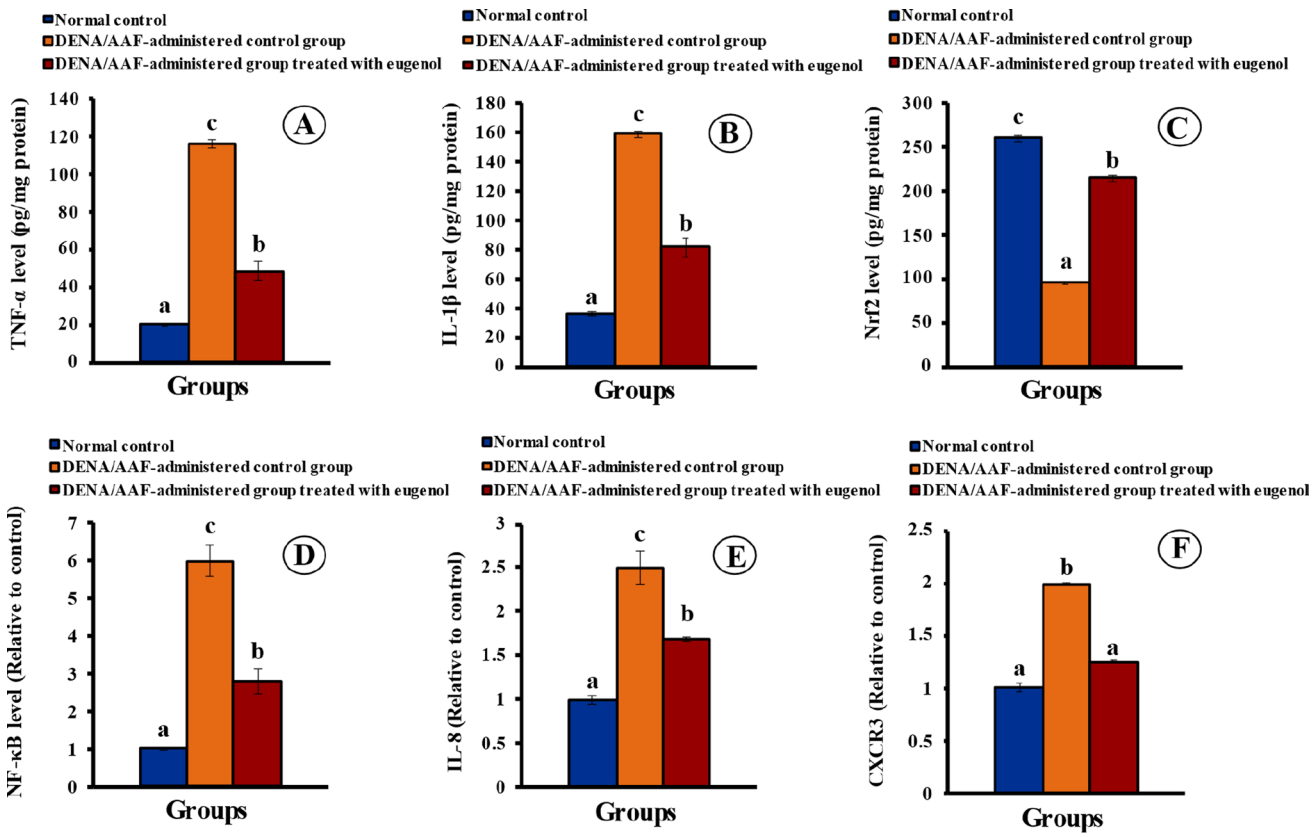

Fig. 6 Effect of eugenol on liver TNF-α (**A**), IL-1β (**B**), and Nrf2 (**C**) levels and NF-κB (**D**), IL-8 (**E**), and CXCR3 (**F**) expression levels in DENA/AAF-administered rats. Values and expressed genes that do not have the same symbol(s) (**a**, **b**, and **c**) are significantly different at $p < 0.05$

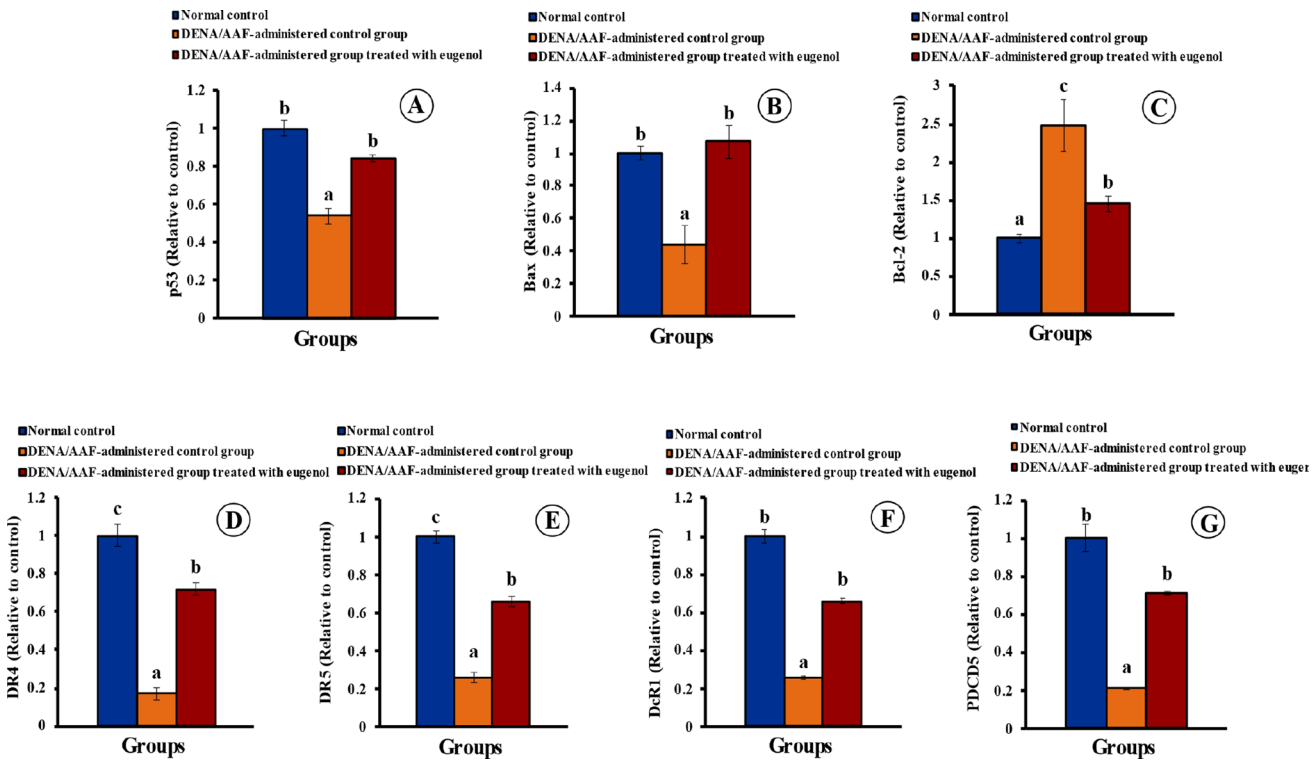

Fig. 7 Effect of eugenol on the expression levels of p53 (**A**), Bax (**B**), Bcl-2 (**C**) DR4 (**D**), DR5 (**E**), DcR1 (**F**), PDCD5 (**G**) in DENA/AAF-administered rats. Values and expressed genes that do not have the same symbol(s) (**a**, **b**, and **c**) are significantly different at $p < 0.05$

3.9 Effect on liver cell migration and division

The administration of DENA/AAF substantially ($p < 0.05$) upregulated the expression of IQ-domain GTPase-activated protein 1 (IQGAP1), IQ-domain GTPase-activated protein 3 (IQGAP3), harvey rat sarcoma viral oncogene homolog (HRAS), kirsten ras oncogene homolog (KRAS), and Ki-67, while substantially ($p < 0.05$) downregulating the expression of IQ-domain GTPase-activated protein 2 (IQGAP2) when compared with the normal control rats. These changes were counteracted by eugenol treatment (Figs. 8 and 9).

4 Discussion

DENA induces HCC as an initiator and AAF as a promoter [39]. The DENA/AAF-triggered HCC model was used in this research to assess ways HCC can avoid the effects of eugenol and to understand its mechanisms of action.

Similar to the outcomes of Ahmed et al. [7] and Tawfik et al. [40], DENA/AAF significantly increased the activities of the cytoplasmic enzyme ALT, the cytoplasmic and mitochondrial enzyme AST, and the membrane-bound enzyme ALP. It also increased bilirubin levels and decreased albumin levels compared with the normal control group. Eugenol was able to significantly reduce the increased activities of ALT, AST, ALP, and the total bilirubin level as well as non-significant albumin. However, eugenol's ability to reduce the increased levels of albumin after DENA/AFF treatment was not statistically significant. DENA/AAF-induced changes in the hepatic membrane were prevented by the membrane stabilizing effect of eugenol, restoring liver integrity, metabolism, and function. These findings agree with those reported by Kumar et al. [41].

The detection of AFP, CA19.9, and CEA is crucial to assess and diagnose HCC [42, 43]. Our results showed that DENA/AAF-administered rats showed elevated serum levels of certain tumor markers due to the induction of liver cancer, which is consistent with the report of Ahmed et al. [7]. Eugenol therapy decreased the raised serum levels of tumor markers in

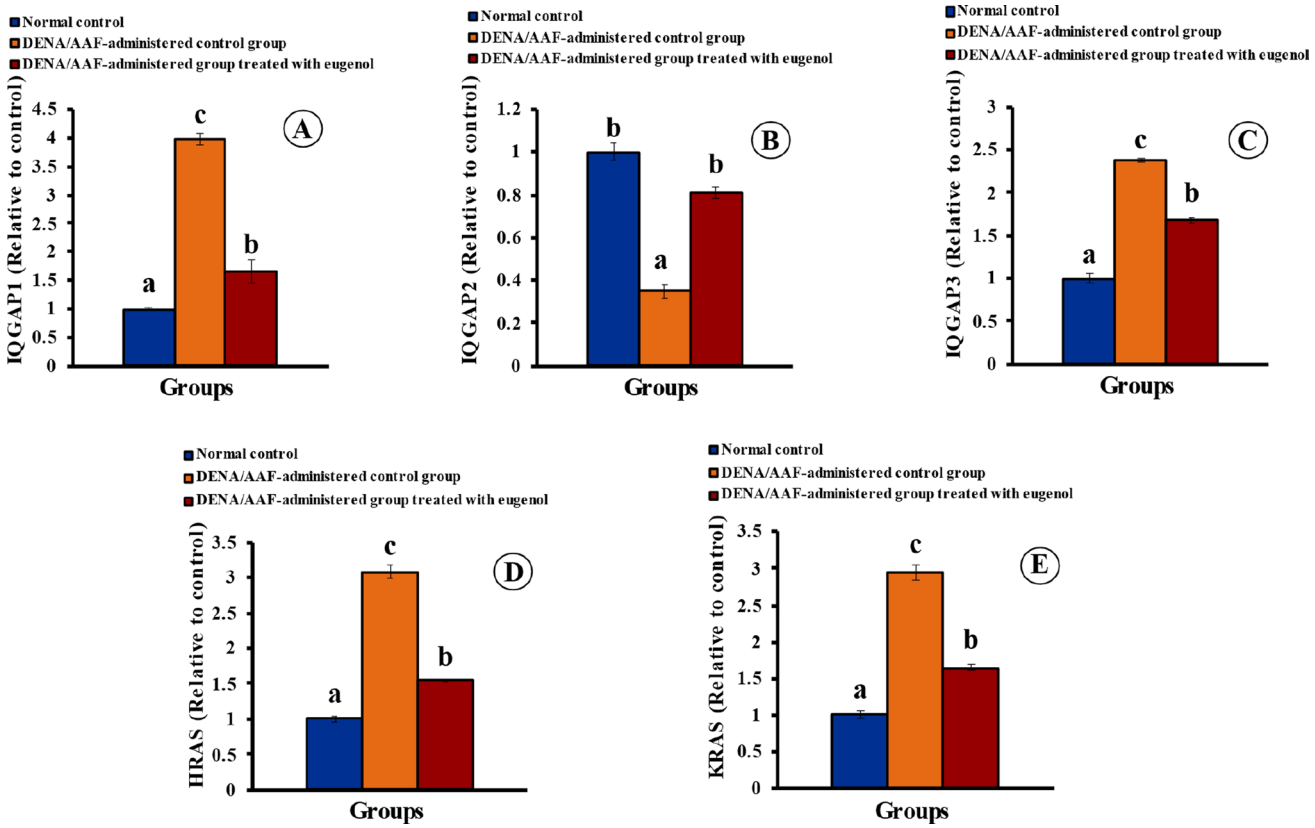

Fig. 8 Effect of eugenol on liver IQGAP1 (**A**), IQGAP2 (**B**), IQGAP3 (**C**), HRAS (**D**), and KRAS (**E**) expression levels in DENA/AAF-administered rats. Values and expressed genes that do not have the same symbol(s) (**a**, **b**, and **c**) are significantly different at $p < 0.05$

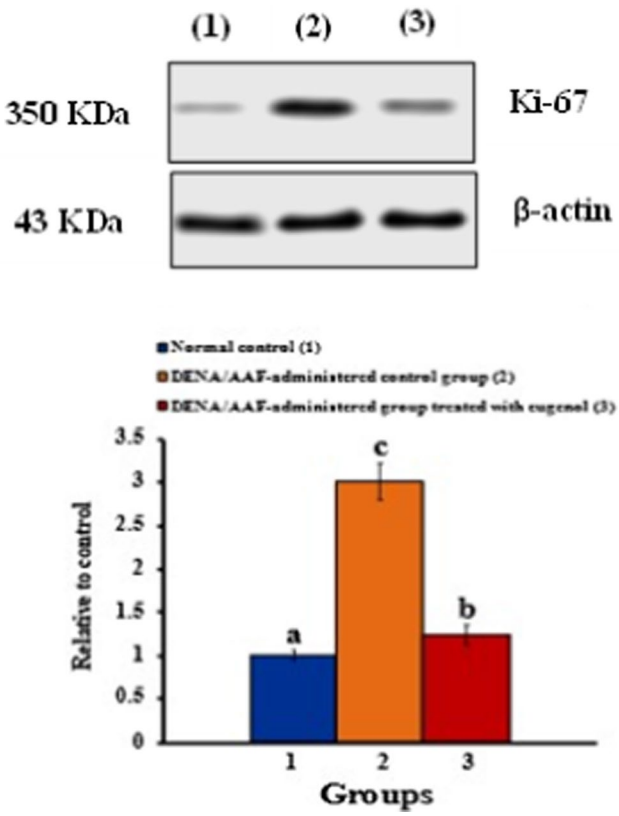

Fig. 9 Effect of eugenol on liver Ki-67 level in DENA/AAF-administered rats. Values and expressed genes that do not have the same symbol(s) (**a**, **b**, and **c**) are significantly different at $p < 0.05$

this DENA/AAF-induced HCC model. Eugenol exerts hepatoprotective activity by protecting the integrity of liver cells and membranes, thereby presenting a lower risk of hepatic injury or HCC [44].

Accompanying the elevated tumor markers, the liver tissue sections displayed necrotic compressed hepatocytes characterized by bile pigment in their cytoplasm, a signet ring appearance, and a binucleated morphology. Tumor cells appeared well-differentiated and resembled nests with peripheral condensed chromatin in disformed nuclei. Apoptotic cells were distinguished by an eosinophilic cytoplasm, blebbing of apoptotic bodies, and condensed chromatin in the nucleus. Like the results of Kumar et al. [41] eugenol treatment significantly reduced necrosis and other histological abnormalities in the liver sections of rats, demonstrating its beneficial effects on the biochemical enzymes involved in liver function and integrity.

DENA/AAF-treated rats exhibited high levels of liver LPO, which is in line with Kaya et al. [45], who suggested that DENA-triggered hepatic damage includes ROS-caused oxidative stress as well as elevated serum and tissue levels of lipid peroxides. DENA/AAF also reduced the activity of the antioxidant enzymes SOD and GPx and the non-enzymatic antioxidant GSH in the liver tissues, in line with the results of Ahmed et al. [7]. Eugenol treatment reduced LPO levels and inhibited the DENA/AAF-stimulated generation of free radicals. Zhang et al. [46] suggests that it may be an effective free radical scavenger which possesses antioxidant potential by disrupting the chain of free radicals and releasing a hydrogen atom. Moreover, in our study, eugenol recovered the decreased SOD and GPx activities and the GSH content in the livers of DENA/AAF-administered rats. Wani et al. [47] proposed that the reduction in oxidative stress following eugenol treatment reflected a putative antioxidant protective function in liver tissue.

NF-κB is a necessary transcription agent in the arrangement of inflammation (Fig. 10), and its disruption contributes to the activation of numerous inflammatory pathways that can lead to cancer [48]. DENA/AAF treatment induced a significant accumulation of inflammatory cytokines TNF-α, IL-1β, and NF-κB relative to the control group. Wu et al. [49] showed that TNF-α can induce the expression of itself and IL-1β by activating NF-κB. Eugenol supplementation dramatically reversed the elevated expression of TNF-α, IL-1β, and NF-κB because of its anti-inflammatory effect. Kaur et al. [50] reported that eugenol's anticarcinogenic action was linked to its anti-inflammatory function, as several inflammation markers were reduced in animals after eugenol treatment (Fig. 10).

In our investigation, DENA/AAF-administered rats showed elevated levels of hepatic IL-8 as a result of induced HCC, consistent with Peng et al. [51]. TNF-α could induce the production of IL-8 from HCC cells by stimulating NF-κB signaling

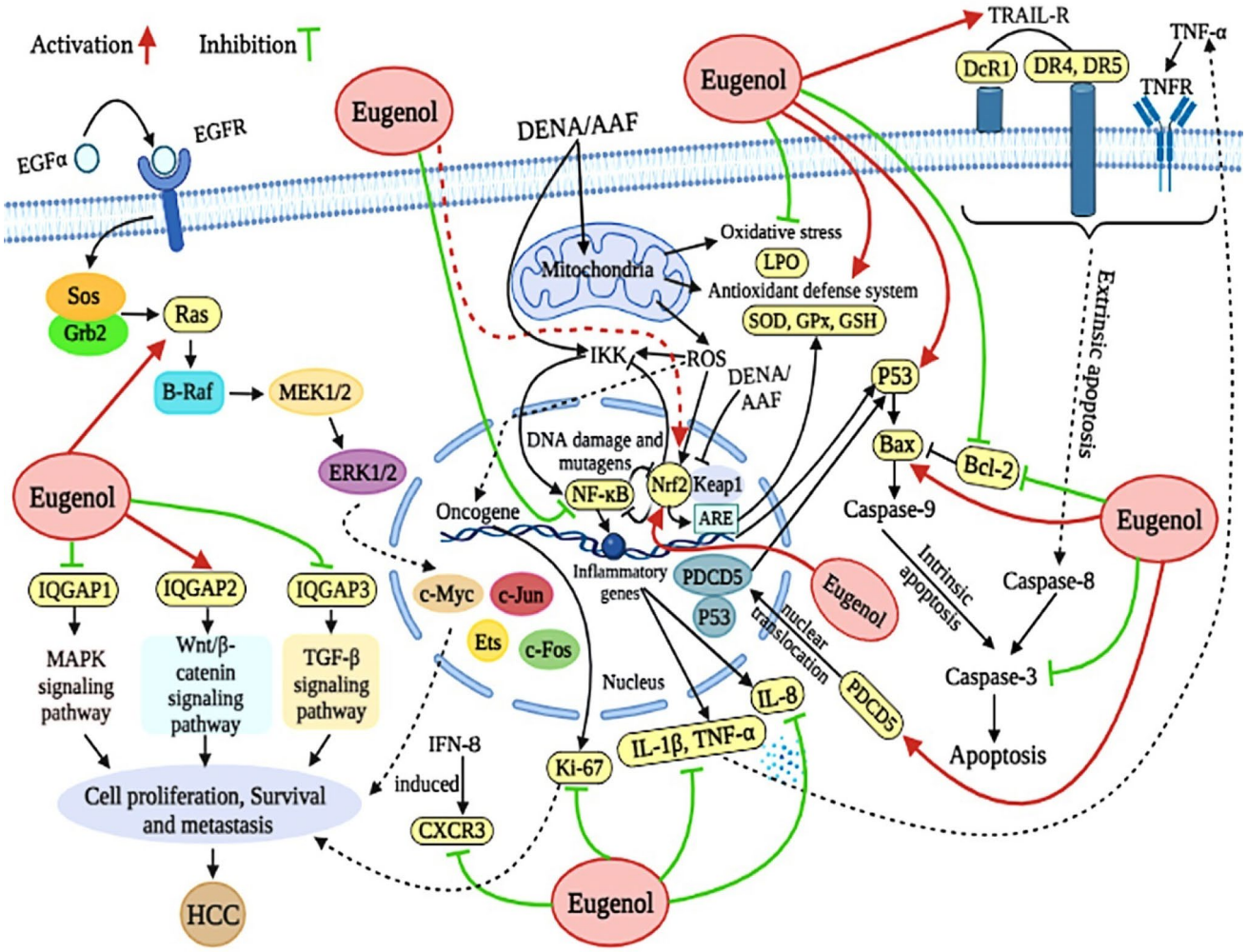

Fig. 10 Schematic figure of eugenol's mechanisms of action in modulating oxidative stress, the antioxidant defense system, migration, inflammation, and apoptosis

pathways [52, 53]. Eugenol treatment significantly decreased IL-8 levels, indicating that eugenol was effective in ameliorating the inflammatory response in DENA/AAF-induced HCC, which is similar to the report by Barboza et al. [54].

Nrf2 is a crucial mediator that is involved in the compensatory mechanism that suppresses ROS levels (Fig. 10). In the current investigation, DENA/AAF administration decreased Nrf2 levels when compared to the normal control group. This is in line with Moon and Giaccia [55] who reported that Nrf2 deficiency causes higher susceptibility to oxidative challenge and carcinogen exposure (Fig. 10). Nrf2 signaling is also involved in attenuating inflammation-associated pathogenesis. Eugenol treatment restored decreased Nrf2 levels, corroborating the results of Ma et al. [56] which stated that eugenol was found to increase the transcriptional activity and expression level of Nrf2, a central regulator of cellular responses to oxidative stress.

DENA/AAF injection increased CXCR3 levels compared to the normal control group. Zhang et al. [57] reported that higher CXCR3 expression is linked to a better therapeutic response in HCC patients. Eugenol treatment lowered the elevated CXCR3 levels [21], validating results that suggest eugenol has anti-inflammatory and anticancer properties.

Here, we demonstrated that DENA/AAF-administered rats exhibited elevated expression of the anti-apoptotic gene Bcl-2 and reduced expression of the pro-apoptotic gene Bax. Bax and Bcl-2 is involved in tumor growth and prognosis in several human cancers. By increasing the mitochondrial outer membrane permeability, causing cytochrome c release into the cytoplasm and subsequently activating caspases, which promote the cleavage of multiple important cellular substrates, leading to cell death. Bcl-2, on the other hand, suppresses apoptosis by reducing Bax activity [58, 59]. DENA/AAF-administered rats also showed reduced p53 gene expression, which is consistent with the results of Zhang and Yu [60]. In the present research, eugenol lowered the expression of Bcl-2 while raising that of both Bax and p53. Thus,

eugenol may produce its anticancer effect, at least in part, via induction of apoptosis in tumor cells (Fig. 10). Jaganathan and Supriyanto [61] found that eugenol induced apoptosis via the mitochondrial pathway and also modulated angiogenesis, invasion, and the expression of Bcl-2 family members. Moreover, Solomon and Abebech [62] proposed that eugenol increases Bax expression, which can enhance mitochondrial cytochrome c release and stimulate the caspase cascade required for cell death. Furthermore, Hussain et al. [63] reported that eugenol's anticancer actions are mediated by its activation of apoptosis and its anti-inflammatory properties.

DENA/AAF-treated rats exhibited a considerable decrease in the expression of DR4, DR5, and DcR1. This finding is consistent with the study by Finnberg et al. [64], which reported that the loss of TRAIL receptors, such as DR4, DR5, and DcR1, promoted neoplastic progression in the liver. Their research suggested that this progression was linked to the inhibition of apoptosis rather than the establishment of preneoplasia associated with DENA-induced DNA damage, and was also connected to unchanged migration in these malignancies. Eugenol-treated rats exhibited elevated levels of DR4, DR5, and DcR1, confirming the findings of Vidhya and Devaraj [65] who suggested that eugenol can inhibit the growth and migration of cancer cells and induce apoptosis (Fig. 10).

DENA/AAF-treated rats exhibited a drop in PDCD5 levels, consistent with the findings of Li et al. [66] who determined that PDCD5 protein stability is essential for apoptosis (Fig. 10). PDCD5 expression has been found to be low in various malignancies. Eugenol-treated rats showed an increase in PDCD5 levels, reflecting its chemopreventive properties. PDCD5 can both expedite apoptosis and trigger multiple other types of cell death in response to various stimuli. PDCD5 passes quickly to the nucleus from the cytoplasm (Fig. 10) in apoptotic cells before phosphatidylserine is externalized and genomic DNA is destroyed [67].

IQGAP genes are important in the development or inhibition of cancer and its progression (Fig. 10) [68]. In this study, DENA/AAF-induced HCC showed elevated levels of IQGAP1 and IQGAP3, along with a decreased level of IQGAP2, compared to the normal control group. These findings suggest that the higher expression of IQGAP1 and IQGAP3, along with the reduced expression of IQGAP2, may be associated with an increased rate of hepatic cancer cell growth and migration. Agustriawan et al. [69] identified IQGAP1 and IQGAP3 as likely oncogenes and IQGAP2 as a tumor suppressor gene. Eugenol treatment downregulated the levels of IQGAP1 and IQGAP3 and upregulated that of IQGAP2, indicating its antiproliferative potential (Fig. 10). Chemoprevention by eugenol decreased cell migration, tumor growth, tumor incidence, and tumor multiplicity [70, 71]. These data are also supported by wound healing assay which show that eugenol contributed to reduce cell migration of HepG2 cell culture.

DENA/AAF-induced HCC was accompanied by a remarkable increase in HRAS and KRAS levels compared with the normal control, mostly because of the elevated cell migration rate. The expression of certain genes was shown to be significantly greater in HCC cells in comparison to normal liver cells; additionally, this increase was more apparent at higher doses of DENA, as reported by Zoheir et al. [72]. Eugenol supplementation ameliorated these raised levels of HRAS and KRAS, demonstrating its antiproliferative effect and supporting the results of Fathy et al. [73] who found that eugenol decreased cell migration rate.

Ki-67 expression is strongly linked to cell migration in tumorigenesis and development, and it is frequently used as a migration marker in pathological studies [73, 74]. In the present investigation, DENA/AAF-administered rats exhibited elevated Ki-67 levels. Mohamedi et al. [75] proposed that elevated Ki-67 expression in cancers is correlated with increased malignancy, increased proclivity for invasion and metastasis, and poor prognosis. Eugenol treatment reduced Ki-67 expression in accordance with its antiproliferative properties. Cassano et al. [76] reported that eugenol addition led to significantly reduced cancer cell migration. However, eugenol, being a natural compound, exhibits a wide range of biological activities. While it has demonstrated potential therapeutic effects, its safety profile requires careful consideration. Eugenol is generally regarded as safe when used at appropriate concentrations, however, excessive doses can result in hepatotoxicity and other adverse effects. Given the role of angiogenesis and lymphangiogenesis in the development of HCC [77, 78], whether Eugenol has potential antiangiogenic and antilymphangiogenic effects warrants future investigation.

In summary, eugenol showed robust prophylactic effects against DENA/AAF-triggered hepatocellular carcinoma and liver injury by inhibiting migration, oxidative stress, and inflammation, while stimulating apoptosis. Additionally, our data gives a new perspective on the mechanics of eugenol in hepatocarcinogenesis treatment through its antioxidant, anti-inflammatory, apoptotic and antiproliferative properties. However, further tests on the efficacy and safety of eugenol in humans, experimental animals, and clinical investigations are required.

Acknowledgements Authors are thankful for Researchers Supporting Project number (RSPD2025R552), King Saud University, Riyadh, Saudi Arabia. The authors are also grateful to Dina Sabry, Medical Biochemistry and Molecular Biology, Faculty of Medicine, Cairo University, Cairo,

Egypt for performing the Western blot analysis. The authors are also grateful to Dr. Sabiha Fatima for her help with the statistical analysis. We would like to sincerely thank Dr. Sabiha Fatima, King Saud University, Riyadh, Saudi Arabia for her invaluable assistance with the statistical analysis in this study.

Author contributions Conceptualization: A.A., K.M.A. and O.M.A.; methodology: H.M.M., A.A., K.M.A., M.Y.Z. and O.M.A.; formal analysis and investigation: H.M.M., A.A., K.M.A., M.Y.Z. and O.M.A.; writing—original draft preparation: H.M.M., A.A., K.M.A., and O.M.A.; writing—review and editing: M.Y.Z., H.M.M., A.A., K.M.A., A.B., M.A.A., A.A., and O.M.A.; funding acquisition: H.M.M., M.A.A., and A.A., resources: H.M.M., and O.M.A.; supervision: A.A., K.M.A. and O.M.A. All authors have read and agreed to the published version of the manuscript.

Funding Open access funding provided by The Science, Technology & Innovation Funding Authority (STDF) in cooperation with The Egyptian Knowledge Bank (EKB). Authors are thankful for Researchers Supporting Project number (RSPD2025R552), King Saud University, Riyadh, Saudi Arabia.

Data availability All data are included in the article.

Declarations

Ethics approval and consent to participate All experiments in the study were approved by Institutional Animal Care and Use Committee (IACUC), Faculty of Science, Beni-Suef University, Egypt (approval number: BSU/FS/2019/3).

Consent for publication The consent for publication has been given by all authors.

Competing interests The authors declare no competing interests.

References

1. Brar G, Kesselman A, Malhotra A, Shah MA. Redefining intermediate-stage HCC treatment in the era of immune therapies. JCO Oncol Pract. 2022;18(1):35–41. https://doi.org/10.1200/op.21.00227.
2. Zamzam ML. Epidemiologic and clinicopathologic features of advanced hepatocellular carcinoma. J Cancer Ther. 2019;10(6):411–21. https://doi.org/10.4236/jct.2019.106034.
3. Liu WT, Jing YY, Gao L, Li R, Yang X, Pan XR, et al. Lipopolysaccharide induces the differentiation of hepatic progenitor cells into myofibroblasts constitutes the hepatocarcinogenesis-associated microenvironment. Cell Death Differ. 2020;27(1):85–101. https://doi.org/10.1038/s41418-019-0340-7.
4. Golemis EA, Scheet P, Beck TN, Scolnick EM, Hunter DJ, Hawk E, et al. Molecular mechanisms of the preventable causes of cancer in the United States. Genes Dev. 2018;32(13–14):868–902. https://doi.org/10.1101/gad.314849.118.
5. Zhou WJ, Huang JT, Lu X, Hu D, Hong X, Wang FA, Lv PH, Zhu XL. Transarterial chemoembolization plus camrelizumab and rivoceranib versus camrelizumab and rivoceranib alone for BCLC Stage C hepatocellular carcinoma. J Hepatocell Carcinoma. 2024;31:2515–24. https://doi.org/10.2147/JHC.S494520.
6. Abdel-Moneim A, Ahmed OM, Abd El-Twab SM, Zaky MY, Bakry LN. Prophylactic effects of *Cynara Scolymus* L leaf and flower hydroethanolic extracts against diethylnitrosamine/acetylaminoflourene-induced lung cancer in wistar rats. Environ Sci Pollut Res. 2021;28(32):43515–27. https://doi.org/10.1007/s11356-021-13391-x.
7. Ahmed OM, Fahim HI, Mohamed EE, Abdel-Moneim A. Protective effects of persea americana fruit and seed extracts against chemically induced liver cancer in rats by enhancing their antioxidant, anti-inflammatory, and apoptotic activities. Environ Sci Pollut Res. 2022;29(29):43858–73. https://doi.org/10.1007/s11356-021-13391-x.
8. You Y, Zhu F, Li Z, Zhang LF, Xie Y, Chinnathambi A, et al. Phyllanthin prevents diethylnitrosamine (DEN) induced liver carcinogenesis in rats and induces apoptotic cell death in HepG2 cells. Biomed Pharmacother. 2021;137: 111335. https://doi.org/10.1016/j.biopha.2021.111335.
9. Zaid OA, Elsonbaty S, Moawad F, Abdelghaffar Mo. Antioxidants and hepatoprotective effects of chitosan nanoparticles against hepatotoxicity induced in rats. Benha Vet Med J. 2019;36(1):252–61. https://doi.org/10.1608/bvmj.2019.111628.
10. Liu Y, Hao C, Li L, Zhang H, Zha W, Ma L, Chen L, Gan J. The role of oxidative stress in the development and therapeutic intervention of hepatocellular carcinoma. Curr cancer Drug Targets. 2023;23(10):792–804. https://doi.org/10.2174/1568009623666230418121130.
11. Shen X, Niu X. Gamma-glutamyl transpeptidase to neutrophil ratio as prognostic indicator for hepatocellular carcinoma patients post-curative resection. J Hepatocellular Carcinoma. 2024;31:2077–85. https://doi.org/10.2147/JHC.S478186.

12. Li Y, Yu Y, Yang L, Wang R. Insights into the role of oxidative stress in hepatocellular carcinoma development. Front Biosci. 2023;28(11):286. https://doi.org/10.31083/j.fbl2811286.
13. Refolo MG, Messa C, Guerra V, Carr BI, D'Alessandro R. Inflammatory mechanisms of HCC development. Cancers. 2020;12(3):641. https://doi.org/10.3390/cancers12030641.
14. Aravalli RN, Cressman EN, Steer CJ. Cellular and molecular mechanisms of hepatocellular carcinoma: an update. Arch toxicol. 2013;87:227–47. https://doi.org/10.1007/s00204-012-0931-2.
15. Abd-Elbaset M, Mansour AM, Ahmed OM, Abo-Youssef AM. The potential chemotherapeutic effect of β-Ionone and/or sorafenib against hepatocellular carcinoma *via* its antioxidant effect, PPAR-γ, FOXO-1, Ki-67, Bax, and Bcl-2 signaling pathways. Naunyn Schmiedebergs Arch Pharmacol. 2020;393(9):1611–24. https://doi.org/10.1007/s00210-020-01863-9.
16. Che L, Paliogiannis P, Cigliano A, Pilo MG, Chen X, Calvisi DF. Pathogenetic, prognostic, and therapeutic role of fatty acid synthase in human hepatocellular carcinoma. Front Oncol. 2019;9:1–10. https://doi.org/10.3389/fonc.2019.01412.
17. Li YK, Wu S, Wu YS, Zhang WH, Wang Y, Li YH, Kang Q, Huang SQ, Zheng K, Jiang GM, Wang QB. Portal venous and hepatic arterial coefficients predict post-hepatectomy overall and recurrence-free survival in patients with hepatocellular carcinoma: a retrospective study. J hepatocellular carcinoma. 2024;31:1389–402. https://doi.org/10.2147/JHC.S462168.
18. Gezici S, Şekeroğlu N. Current perspectives in the application of medicinal plants against cancer: novel therapeutic agents. Anticancer Agents Med Chem. 2019;19(1):101–11. https://doi.org/10.2174/1871520619666181224121004.
19. Makuch E, Nowak A, Günther A, Pełech R, Kucharski Ł, Duchnik W, et al. The effect of cream and gel vehicles on the percutaneous absorption and skin retention of a new eugenol derivative with antioxidant activity. Front Pharmacol. 2021;12:1–13. https://doi.org/10.3389/fphar.2021.658381.
20. Aburel OM, Pavel IZ, Dănilă MD, Lelcu T, Roi A, Lighezan R, et al. Pleiotropic effects of eugenol: the good, the bad, and the unknown. Oxid Med Cell Longev. 2021;2021:1–15. https://doi.org/10.1155/2021/3165159.
21. Zari AT, Zari TA, Hakeem KR. Anticancer properties of eugenol: a review. Molecules. 2021;26(23):7407. https://doi.org/10.3390/molecules26237407.
22. Sun X, Veeraraghavan VP, Surapaneni KM, Hussain S, Mathanmohun M, Alharbi SA, et al. Eugenol-piperine loaded polyhydroxy butyrate/polyethylene glycol nanocomposite-induced apoptosis and cell death in nasopharyngeal cancer (C666–1) cells through the inhibition of the PI3K/AKT/MTOR signaling pathway. J Biochem Mol Toxicol. 2021;35(4): e22700. https://doi.org/10.1002/jbt.22700.
23. Abdullah ML, Al-Shabanah O, Hassan ZK, Hafez MM. Eugenol-induced autophagy and apoptosis in breast cancer cells via Pi3k/Akt/Foxo3a pathway inhibition. Int J Mol Sci. 2021;22(17):9243. https://doi.org/10.3390/ijms22179243.
24. Yassin NYS, AbouZid SF, El-Kalaawy AM, Ali TM, Almehmadi MM, Ahmed OM. Silybum marianum total extract, silymarin and silibinin abate hepatocarcinogenesis and hepatocellular carcinoma growth *via* modulation of the HGF/c-Met, Wnt/β-Catenin, and PI3K/Akt/MTOR signaling pathways. Biomed Pharmacother. 2022;145: 112409. https://doi.org/10.1016/j.biopha.2021.112409.
25. Mosmann T. Rapid colorimetric assay for cellular growth and survival: application to proliferation and cytotoxicity assays. J Immunol Methods. 1983;145: 112409.
26. Martinotti S, Ranzato E. Scratch wound healing assay. Epidermal Cells Methods Protoc. 2020;2109:225–9.
27. de Luján AM, Cerliani JP, Monti J, Carnovale C, Ronco MT, Pisani G, et al. The in vivo apoptotic effect of interferon Alfa-2b on rat preneoplastic liver involves Bax protein. Hepatology. 2002;35(4):824–33. https://doi.org/10.1053/jhep.2002.32099.
28. Ferland CE, Beaudry F, Vachon P. Antinociceptive effects of eugenol evaluated in a monoiodoacetate-induced osteoarthritis rat model. Phyther Res. 2012;26(9):1278–85. https://doi.org/10.1002/ptr.3725.
29. Gella FJ, Olivella T, Pastor MC, Arenas J, Moreno R, Durban R, et al. A simple procedure for the routine determination of aspartate aminotransferase and alanine aminotransferase with pyridoxal phosphate. Clin Chim Acta. 1985;153(3):241–7. https://doi.org/10.1016/0009-8981(85)90358-4.
30. Schumann G, Klauke R, Canalias F, Bossert-Reuther S, Franck PFH, Gella FJ, et al. IFCC primary reference procedures for the measurement of catalytic activity concentrations of enzymes at 37°C part 9: reference procedure for the measurement of catalytic concentration of alkaline phosphatase international federation of clinical chemistr. Clin Chem Lab Med. 2011;49(9):1439–46. https://doi.org/10.1515/CCLM.2011.621.
31. Jendrassik L. Colorimetric determination of bilirubin. Biochemistry. 1938;97:72–81.
32. Doumas BT, Watson WA, Biggs HG. Albumin standards and the measurement of serum albumin with bromcresol green. Clin Chim Acta. 1971;31(1):87–96. https://doi.org/10.1016/0009-8981(71)90365-2.
33. Ohkawa H, Ohishi N, Yagi K. Assay for lipid peroxides in animal tissues by thiobarbituric acid reaction. Anal Biochem. 1979;95(2):351–8. https://doi.org/10.1016/0003-2697(79)90738-3.
34. Beutler E, Duron O, Kelly B. Improved method for the determination of blood glutathione. J Lab Clin Med. 1963;61:882–8.
35. Paglia DE, Valentine WN. Studies on the quantitative and qualitative characterization of erythrocyte glutathione peroxidase. J Lab Clin Med. 1967;70(1):158–69.
36. Nishikimi M, Roa N, Yogi K. Measurement of superoxide dismutase. Biochem Biophys Res Commun. 1972;46:849–54.
37. Ragab TIM, Zoheir KMA, Mohamed NA, El Gendy AENG, Abd-ElGawad AM, Abdelhameed MF, et al. Cytoprotective potentialities of carvacrol and its nanoemulsion against cisplatin-induced nephrotoxicity in rats: development of nano-encasulation form. Heliyon. 2022;8(3): e09198. https://doi.org/10.1016/j.heliyon.2022.e09198.
38. Banchroft J, Stevens A, Turner D. Theory and practice of histological techniques. New York: Churchil Livingstone; 1996.
39. Gholibeikian M, Arvaneh A. Synthesis, cytotoxicity of carnosine peptide analogues on mitochondria obtained from cancerous rats' liver. J Org Chem Synth Process Dev. 2021;1(1):1–11.
40. Tawfik NG, Mohamed WR, Mahmoud HS, Alqarni MA, Naguib IA, Fahmy AM, et al. Isatin counteracts diethylnitrosamine/2-acetylaminofluorene-induced hepatocarcinogenesis in male wistar rats by upregulating anti-inflammatory, antioxidant, and detoxification pathways. Antioxidants. 2022;11(4):699. https://doi.org/10.3390/antiox11040699.
41. Kumar A, Siddiqi NJ, Alrashood ST, Khan HA, Dubey A, Sharma B. Protective effect of eugenol on hepatic inflammation and oxidative stress induced by cadmium in male rats. Biomed Pharmacother. 2021;139: 111588. https://doi.org/10.1016/j.biopha.2021.111588.

42. Li Y, Li DJ, Chen J, Liu W, Li JW, Jiang P, et al. Application of joint detection of AFP, CA19-9, CA125 and CEA in identification and diagnosis of cholangiocarcinoma. Asian Pacif J Cancer Prev. 2015;16(8):3451–5. https://doi.org/10.7314/APJCP.2015.16.8.3451.
43. Lin KY, Zhang JX, Lin ZW, Chen QJ, Luo LP, Chen JH, Wang K, Tai S, Zhang ZB, Wang SF, Li JD. Serum alpha-fetoprotein response as a preoperative prognostic indicator in unresectable hepatocellular carcinoma with salvage hepatectomy following conversion therapy: a multicenter retrospective study. Front Immunol. 2024;16(15):1308543. https://doi.org/10.3389/fimmu.2024.1308543.
44. Yildiz H, Ozturk E. Histopathological and Biochemical effects of eugenol on alcohol-treated rat liver Adıyaman. Univ J Sci. 2020;10(1):83–99. https://doi.org/10.37094/adyujsci.729426.
45. Kaya E, Yilmaz S, Çeribaşi AO, Telo S. Protective effect of lycopene on diethylnitrosamine-induced oxidative stress and catalase expression in rats. Ankara Univ Vet Fak Derg. 2019;66(1):43–52. https://doi.org/10.1501/Vetfak_0000002886.
46. Zhang LL, Zhang LF, Xu JG, Hu QP. Comparison study on antioxidant, DNA damage protective and antibacterial activities of eugenol and isoeugenol against several foodborne pathogens. Food Nutr Res. 2017;61(1):1353356. https://doi.org/10.1080/16546628.2017.1353356.
47. Wani MR, Maheshwari N, Shadab G. Eugenol attenuates TiO2 Nanoparticles-induced oxidative damage, biochemical toxicity and DNA damage in wistar rats: an in vivo study. Environ Sci Pollut Res. 2021;28(18):22664–78. https://doi.org/10.1007/s11356-020-12139-3.
48. Kundaktepe BP, Sozer V, Kocael PC, Durmus S, Kurtulus D, Papila C, et al. Circulating nuclear factor-kappa b mediates cancer-associated inflammation in human breast and colon cancer. J Med Biochem. 2021;40(2):150–9. https://doi.org/10.5937/jomb0-27128.
49. Wu C, Fernandez SA, Criswell T, Chidiac T, Guttridge D, Villalona-Calero M, et al. Disrupting cytokine signaling in pancreatic cancer a phase I/II study of etanercept in combination with gemcitabine in patients with advanced disease. Pancreas. 2013;42(5):813–8. https://doi.org/10.1097/MPA.0b013e318279b87f.
50. Kaur G, Athar M, Sarwar AM. Eugenol precludes cutaneous chemical carcinogenesis in mouse by preventing oxidative stress and inflammation and by inducing apoptosis. Mol Carcinog. 2010;49(3):290–301. https://doi.org/10.1002/mc.20601.
51. Peng S, Chen Y, Gong Y, Li Z, Xie R, Lin Y, et al. Predictive value of intratumour inflammatory cytokine Mrna levels of hepatocellular carcinoma patients and activation of two distinct pathways govern IL-8 induced epithelial-mesenchymal transition in human hepatic cancer cell lines. Cytokine. 2019;119:81–9. https://doi.org/10.1016/j.cyto.2019.03.012.
52. Wang Y, Wang W, Wang L, Wang X, Xia J. Regulatory mechanisms of interleukin-8 production induced by tumour necrosis factor-α in human hepatocellular carcinoma cells. J Cell Mol Med. 2012;16(3):496–506. https://doi.org/10.1111/j.1582-4934.2011.01337.x.
53. Zhu B, Gao F, Li Y, Shi K, Hou Y, Chen J, Zhang Q, Wang X. Serum cytokine and chemokine profiles and disease prognosis in hepatitis B virus-related acute-on-chronic liver failure. Front Immunol. 2023;27(14):1133656. https://doi.org/10.3389/fimmu.2023.1133656.
54. Barboza JN, Filho CSMB, Silva RO, Medeiros JVR, de Sousa DP. An overview on the anti-inflammatory potential and antioxidant profile of eugenol. Oxid Med Cell Longev. 2018. https://doi.org/10.1155/2018/3957262.
55. Moon E, Giaccia A. Dual roles of Nrf2 in tumor prevention and progression: possible implications in cancer treatment. Free Radic Biol Med. 2015;79:292–9. https://doi.org/10.1016/j.freeradbiomed.2014.11.009.
56. Ma L, Liu J, Lin Q, Gu Y, Yu W. Eugenol protects cells against oxidative stress *via* Nrf2. Exp Ther Med. 2020;21(2):1–8. https://doi.org/10.3892/etm.2020.9539.
57. Zhang J, Chen J, Guan G, Zhang T, Lu F, Chen X. Expression and clinical significance of chemokine CXCL10 and its receptor CXCR3 in hepatocellular carcinoma. J Peking Univ Heal Sci. 2019;51(3):402–8. https://doi.org/10.19723/j.issn.1671-167x.2019.03.005.
58. Hector S, Prehn JHM. Apoptosis signaling proteins as prognostic biomarkers in colorectal cancer: a review. Biochim Biophys Acta—Rev Cancer. 2009;1795(2):117–29. https://doi.org/10.1016/j.bbcan.2008.12.002.
59. Mohan S, Abdelwahab SI, Kamalidehghan B, Syam S, May KS, Harmal NSM, et al. Involvement of NF-κB and Bcl2/Bax signaling pathways in the apoptosis of MCF7 cells induced by a xanthone compound pyranocycloartobiloxanthone A. Phytomedicine. 2012;19(11):1007–15. https://doi.org/10.1016/j.phymed.2012.05.012.
60. Zhang X, Yu H. Matrine inhibits diethylnitrosamine-induced HCC proliferation in rats through inducing apoptosis *via* P53, Bax-dependent caspase-3 activation pathway and down-regulating MLCK overexpression. Iran J Pharm Res. 2016;15(2):491–9.
61. Jaganathan S, Supriyanto E. Antiproliferative and molecular mechanism of eugenol-induced apoptosis in cancer cells. Molecules. 2012;17(6):6290–304. https://doi.org/10.3390/molecules17066290.
62. Solomon H, Abebech B. Natural therapies of the inflammatory bowel disease: the case of rutin and its aglycone. Quercetin Mini Rev Med Chem. 2018;18(3):234–43. https://doi.org/10.2174/1389557517666170120152417.
63. Hussain A, Brahmbhatt K, Priyani A, Ahmed M, Rizvi TA, Sharma C. Eugenol enhances the chemotherapeutic potential of gemcitabine and induces anticarcinogenic and anti-inflammatory activity in human cervical cancer cells. Cancer Biother Radiopharm. 2011;26(5):519–27. https://doi.org/10.1089/cbr.2010.0925.
64. Finnberg N, Klein-Szanto AJP, El-Deiry WS. TRAIL-R deficiency in mice promotes susceptibility to chronic inflammation and tumorigenesis. J Clin Investig. 2008;118(1):111–23. https://doi.org/10.1172/JCI29900.
65. Vidhya N, Devaraj SN. Induction of apoptosis by eugenol in human breast cancer cells. Indian J Exp Biol. 2011;49(11):871–8.
66. Li H, Wang Q, Gao F, Zhu F, Wang X, Zhou C, et al. Reduced expression of PDCD5 is associated with high-grade astrocytic gliomas. Oncol Rep. 2008;20:573–9. https://doi.org/10.3892/or_00000044.
67. Chen Y, Li G. PDCD5 (Programmed cell death 5). Atlas Genet Cytogenet Oncol Haematol. 2017;19:621–4. https://doi.org/10.4267/2042/62481.
68. Zoheir KMA, Abd-Rabou AA, Harisa GI, Ashour AE, Ahmad SF, Attia SM, et al. Gene expression of IQGAPs and Ras families in an experimental mouse model for hepatocellular carcinoma: a mechanistic study of cancer progression. Int J Clin Exp Pathol. 2015;8(8):8821–31.
69. Agustriawan D, Sumarpo A, Parikesit AA, Nurdiansyah R, Adisurja GP, Fajar Ap RR. In silico study of mirna-regulated IQ motif-containing gtpase-activating protein family in liver cancer. Asian J Pharm Clin Res. 2018;11:98–101. https://doi.org/10.22159/ajpcr.2018.v11s3.30046.
70. Manikandan P, Vinothini G, Priyadarsini RV, Prathiba D, Nagini S. eugenol inhibits cell proliferation *via* NF-κB suppression in a rat model of gastric carcinogenesis induced by MNNG. Invest New Drugs. 2011;29(1):110–7. https://doi.org/10.1007/s10637-009-9345-2.
71. Jaganathan SK, Mazumdar A, Mondhe D, Mandal M. Apoptotic effect of eugenol in human colon cancer cell lines. Cell Biol Int. 2011;35(6):607–15. https://doi.org/10.1042/cbi20100118.
72. Fathy M, Fawzy MA, Hintzsche H, Nikaido T, Dandekar T, Othman EM. Eugenol exerts apoptotic effect and modulates the sensitivity of HeLa cells to cisplatin and radiation. Molecules. 2019;24(21):3979. https://doi.org/10.3390/molecules24213979.

73. Li LT, Jiang G, Chen Q, Zheng JN. Predic Ki67 is a promising molecular target in the diagnosis of cancer (review). Mol Med Rep. 2015;11(3):1566–72. https://doi.org/10.3892/mmr.2014.2914.
74. Zhang W, Zhou Q, Liu H, Xu J, Huang R, Shen B, Guo Y, Ai X, Xu J, Zhao X, Liu Y. Bacteroides fragilis strain ZY-312 facilitates colonic mucosa regeneration in colitis via motivating STAT3 signaling pathway induced by IL-22 from ILC3 secretion. Front Immunol. 2023;11(14):1156762.
75. Mohamedi Y, Fontanil T, Solares L, Garcia-Suárez O, García-Piqueras J, Vega JA, et al. Fibulin-5 downregulates Ki-67 and inhibits proliferation and invasion of breast cancer cells. Int J Oncol. 2016;48(4):1447–56. https://doi.org/10.3892/ijo.2016.3394.
76. Cassano R, Cuconato M, Calviello G, Serini S, Trombino S. Recent advances in nanotechnology for the treatment of melanoma. Molecules. 2021;26(4):785. https://doi.org/10.3390/molecules26040785.
77. Li J, Wang QB, Liang YB, Chen XM, Luo WL, Li YK, Chen X, Lu QY, Ke Y. Tumor-associated lymphatic vessel density is a reliable biomarker for prognosis of esophageal cancer after radical resection: a systemic review and meta-analysis. Front Immunol. 2024;20(15):1453482. https://doi.org/10.3389/fimmu.2024.1453482.
78. Thelen A, Jonas S, Benckert C, Weichert W, Schott E, Bötcher C, Dietz E, Wiedenmann B, Neuhaus P, Scholz A. Tumor-associated lymphangiogenesis correlates with prognosis after resection of human hepatocellular carcinoma. Ann surg oncol. 2009;16:1222–30. https://doi.org/10.1245/s10434-009-0380-1.